Transport and Communications Science Journal, Vol. 75, Issue 4 (05/2024), 1502-1517

Transport and Communications Science Journal

DEVELOPMENT OF AN ARTIFICIAL NEURAL NETWORK BASED-PREDICTION MODEL FOR BOND STRENGTH OF FRP BARS IN CONCRETE

Huynh Phuong Nam[1], Tran Le Anh Duc[1], Phan Hoang Nam[1*], Nguyen Minh Hai[1], Phan Da Thao[2]

[1]The University of Danang – University of Science and Technology, No 54 Nguyen Luong Bang Street, Danang, Vietnam

[2]The College of Technology, Economics and Irrigation Central, No 14 Nguyen Tat Thanh Street, Hoian, Quangnam, Vietnam

ARTICLE INFO

TYPE: Research Article
Received: 14/12/2023
Revised: 23/04/2024
Accepted: 15/04/2024
Published online: 15/05/2024
https://doi.org/10.47869/tcsj.75.4.3
[*] *Corresponding author*
Email: phnam@dut.udn.vn; Tel: +84931225799

Abstract. Fiber-reinforced polymer (FRP) bars have garnered increasing attention in recent years due to their superior corrosion resistance, offering a potential solution to the significant drawback of steel corrosion in concrete. For the widespread utilization of FRP bars in concrete structures, determining the bond strength between FRP bars and concrete is a crucial topic. This study seeks to develop a prediction model to estimate the bond strength of FRP bars in concrete, utilizing an extended dataset from 1010 pull-out tests. Initially, the study evaluates the applicability of several bond strength formulas from existing codes. Subsequently, two prediction models, namely a multivariate linear regression model and an artificial neural network (ANN) model, are introduced for estimating the bond strength of FRP bars in concrete. The results indicate that the correlation between the evaluation values of existing formulas and the experimental value is very low. This is because these formulas have not yet been updated to encompass the expanded usage scopes of FRP bars with various surface processing methods and types of concrete. While the multivariate linear regression model outperforms these formulas, its accuracy is still relatively low; in contrast, the ANN demonstrates superior performance, achieving an R^2 value for both the validation and test set of more than 0.92. The findings highlight that, when considering a broader range of applications, the ANN serves as a robust tool for accurately predicting the bond strength of FRP bars in concrete, in comparison to traditional formulas and linear regression models. This assessment approach provides engineers with a convenient, high-precision tool for designs utilizing various forms of FRP bars and diverse types of concrete in practical design scenarios.

Keywords: fiber-reinforced polymer bar; pull-out test; bond strength; ANN model; machine learning technique.

1. INTRODUCTION

FRP (fiber-reinforced polymer) composites are crafted by integrating Carbon (C), Glass (G), or Basalt (B) fibers into polymer resins, namely polyester, vinylester, or epoxy, which serve as the matrix binding the fibers into cohesive composites. These synthetic materials exhibit remarkable properties, including corrosion resistance, high tensile strength, elevated fatigue resistance, a weight advantage of approximately 25% compared to steel reinforcement, and ease of processing. Consequently, this material is increasingly gaining prominence in both Vietnam and globally [1].

While the predominant applications currently involve FRP panels reinforcing steel or concrete structures [1, 2], there is a recent shift towards exploring FRP bars as a potential solution for either complete or partial replacement of steel reinforcement within reinforced concrete structures. This alternative aligns with durability requirements and proves suitable for construction projects in regions characterized by harsh environmental conditions and heightened steel corrosion rates [3-6]. To facilitate the widespread development of FRP bar-reinforced concrete structures, beyond optimizing the production process to minimize the cost of FRP materials, it is imperative to accurately determine the fundamental characteristics of FRP bars, particularly when utilized within concrete applications.

In FRP-reinforced concrete structures, a critical parameter to ascertain is the bond strength between FRP reinforcement and concrete. While RC structures exhibit near-rigid integration between steel bars and concrete [7], the bond strength between the FRP bar and concrete in FRP-reinforced concrete structures is usually lower, and the slip between the two materials cannot be ignored during the design calculation. This bond behavior depends on various parameters such as fiber type, surface treatment, diameter and strength of the FRP bar, strength of concrete, structural component size, and boundary and loading conditions [8-10]. Thus, a precise assessment of the bond strength between FRP bars and concrete is essential, aiding engineers in enhancing the accuracy of calculations for FRP bar-reinforced concrete structures, while considering the slip behavior of bars in concrete [11-14].

Many studies are focusing on evaluating the bond behavior between FRP bars and concrete. Empirical formulas have been proposed in previous studies [15, 16], and design codes such as ACI [17], CSA [18, 19], JSCE [20], and FIB [21] have been established to evaluate FRP bar bond strength in concrete. Each formula is constructed based on a specific set of experimental data and with a certain range of parameters such as fiber type, surface treatment method, FRP bar diameter, and concrete strength. Meanwhile, machine learning techniques are also utilized to train optimal models for evaluating FRP-concrete bond strength based on experimental databases. Notably, Nolan et al. [22] introduced a method to estimate FRP bond strength in concrete through artificial neural networks, achieving an impressive R-value of 0.982 based on 184 experimental specimens; however, it considered only seven input variables. In a similar vein, Bogachan et al. [23] compared bond strength evaluations derived from different design formulas and machine learning techniques, encompassing artificial neural networks, support vector methods, and multivariate linear regression models. However, these studies focused on a limited range of FRP bar diameter, concrete strength, FRP fiber type, and particularly surface treatment methods for specific types of FRP bars.

In recent years, advancements in FRP composite material technology have led to the development of various surface treatment techniques for bonding FRP bars with concrete, including fine sand coated, rough sand coated, helically wrapped, braided, grooved, and smooth

surfaces [24-29]. Some studies have also combined two or more of these surface treatments. The surface treatment of FRP bars significantly affects the stress transfer ability between the FRP bars and concrete, thereby influencing the bond behavior between the two materials. However, most previous studies have only evaluated the bond strength of FRP bars with one or a small number of surface types [15-18, 20-23]. Therefore, in the preliminary design process of FRP bar-reinforced concrete structures, engineers need to consult multiple models or evaluation formulas while understanding the conditions and scope of each. In many cases, engineers need to compare the correlation between experimental models and real-world usage conditions. This can be a challenge as information must be gathered from numerous studies and models. Therefore, developing a comprehensive model that evaluates the bond strength of various types of FRP bars in concrete, including multiple surface treatment methods and a broad application range of fiber type, concrete strength, and FRP bar diameter, can help engineers save time in the preliminary design stages.

This study seeks to introduce a more comprehensive assessment method than previous endeavors, particularly concerning the bond strength of FRP bars with various surface types within concrete, spanning normal, high-strength, and ultra-high-strength concrete. To achieve this objective, regression models, including multivariate linear regression (MLR) and artificial neural networks (ANN), are employed to evaluate bonding strength based on datasets derived from related experiments, totaling 1010 samples encompassing different types of FRP bars [15, 16, 30-60]. The dataset used in the model incorporates parameters such as FRP bar type, bar covering surface, bar diameter, elastic modulus, buried length of FRP bar, and compressive strength of concrete, with the output parameter being bond strength. Comparative results from the ANN model and multivariate regression against experimental outcomes allow for a nuanced assessment of the applicability of each model.

2. STRUCTURE OF DATASET

A dataset comprising 1010 specimens, sourced from 32 studies, was chosen [15, 16, 30-60]. There are numerous experimental methods to evaluate the bond strength of FRP bars in concrete; however, to limit the influence of experimental methods, the collected dataset focused solely on the pull-out test, which is a commonly used method for evaluating the bond strength between FRP bars and concrete. In this experimental setup, the FRP bar is embedded in concrete, with the concrete size adjusted according to the diameter of the FRP bar. To mitigate the influence of the uneven stress distribution phenomenon along the entire length of the bar, a part of the bar's surface undergoes treatment to omit the bond between the concrete and FRP bar. The bond strength between the FRP bar and concrete is quantified as the maximum tensile force divided by the contact surface area of the FRP bar in contact with the concrete.

The dataset consists of 9 input variables and the corresponding output, representing bond strength. Figure 1 visually depicts the data distribution for each numeric variable through histograms, highlighting key statistical measures such as the maximum, minimum, mean, and standard deviation (std). Meanwhile, Figure 2 provides an overview of the dataset's structure, focusing on labeled variables like FRP fiber type, surface treatment method, and observed failure modes in pull-out tests.

Examining the figures, it is evident that the typical application range for concrete compressive strengths spans from 30 MPa to 60 MPa, while bar diameters vary from 8 to 20 mm. The elastic modulus of bars falls between 40 to 60 GPa, with tensile strength ranging from 600 to 800 MPa and 1000 to 1200 MPa. However, the dataset displays an uneven distribution

for certain parameters, such as fiber type, resin type, surface treatment, and failure modes. Notably, GFRP-type FRP bars constitute the majority, making up 69% of the experimental data, surpassing other types of bars.

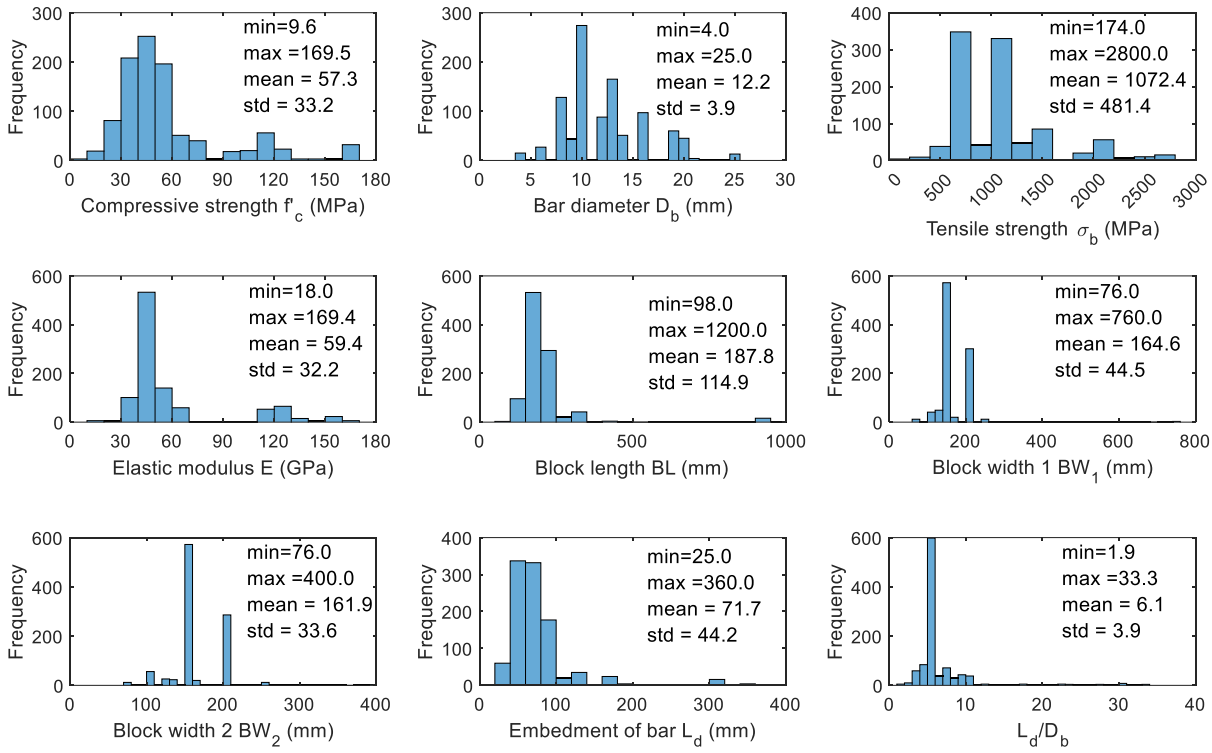

Figure 1. Illustation of the numeric input variables.

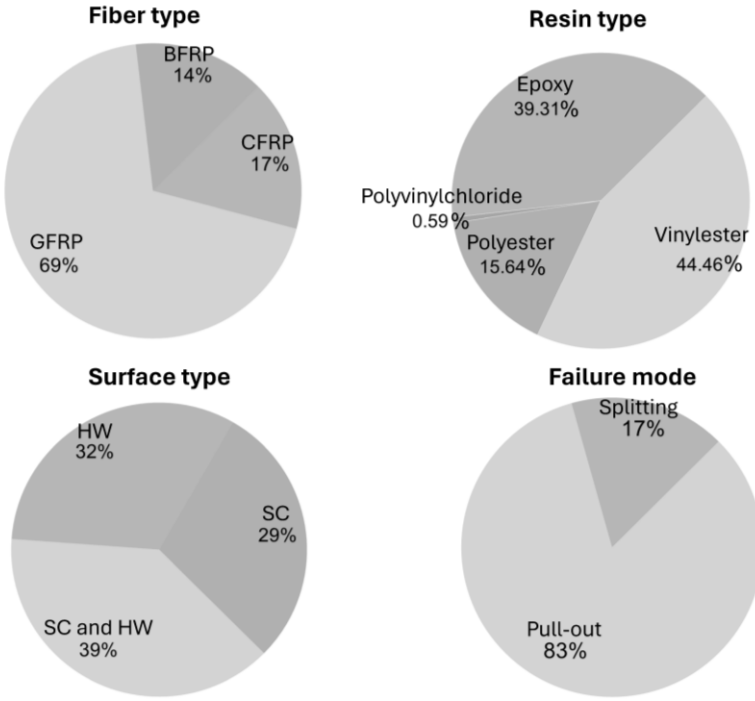

Figure 2. Illustration of the labeled input variables.

Additionally, the dataset reveals that the epoxy and vinylester resins account for more than 83%, and surface treatment methods, including sand-coated (SC) machining, helically wrapped (HW), and the combination of both (HW and SC), are commonly employed. Moreover, pull-out failure predominates in the dataset, accounting for 83% of cases compared to concrete splitting failure.

3. APPLICABILITY OF EXISTING FORMULAS FOR BOND STRENGTH OF FRP BARS IN CONCRETE

3.1. Existing formulas of bond strength

Before constructing the prediction model, an analysis comparing the correlation between the experimental results from the dataset and the proposed experimental formulas in design codes was conducted. Table 1 presents five such formulas specified in existing codes. The formulas specified in the FIB code [21] have a simple structure, primarily evaluating the bond strength of FRP bars in concrete based on the compressive strength of the concrete. On the other hand, the formulas specified in the design codes of ACI [17], CSA [18, 19], and JSCE [20] are more complex. The ACI 440.1R-06 formula takes into consideration factors such as the size of the concrete cover block and the length of the embedded part of the FRP bar in concrete. The CSA-S806 formulas also consider similar factors along with other variables like the relative position of the FRP bar arrangement inside the concrete block, the type of fiber, and surface treatment methods through influencing coefficients. The JSCE formula considers a coefficient that reflects the confined effect of the surrounding concrete.

Table 1. Previous empirical formulas for the bond strength of FRP bars and concrete.

References	Formula
ACI 440.1R-06 [17]	$\frac{\tau_b}{0.083\sqrt{f_c}} = 4.0 + 0.3\frac{C}{d_b} + 100\frac{d_b}{l_d}$
CSA-S806 [18]	$\tau_b = \frac{C\sqrt{f_c}}{1.15(K_1K_2K_3K_4K_5)\pi d_b}$
CSA S6-06 [19]	$\tau_b = \frac{0.4C\sqrt{f_c}}{0.45\pi d_b K_1K_4}$
JSCE [20]	$\tau_b = \frac{f_{bod}}{\alpha_1} = \frac{0{,}28\, f_c^{2/3}}{1.3\ \alpha_1}$ α_1 depends on $k_c = \frac{C}{d_b} + \frac{15A_t}{sd_b}$, in detail: $\alpha_1 = 1.0$ when $k_c \le 1.0$; $\alpha_1 = 0.9$ when $1.0 < k_c \le 1.5$; $\alpha_1 = 0.8$ when $1.5 < k_c \le 2.0$; $\alpha_1 = 0.7$ when $2.0 < k_c \le 2.5$; $\alpha_1 = 0.6$ when $2.5 \le k_c$
FIB [21]	$\tau_b = \gamma\sqrt{f_c}$

Notes: τ_b: Bond strength (MPa); f_c: Concrete compressive strength (MPa); C: Smallest cover to the bar or one-half of the center-on-center spacing of the bars (mm); d_b: Bar diameter (mm); l_d: Embedded length of the bar in concrete (mm); K_1: Bar location factor (1.3 for horizontal bar placed more than 300 mm of fresh concrete is cast below the bar, 1.0 for all other

cases); K_2: Concrete density factor (1.3 for low-density concrete, 1.2 for semi-low-density concrete, 1.0 for normal-density concrete); K_3: Bar size factor (0.8 for A_b ≤300 mm^2, 1.0 for A_b > 300 mm^2, with A_b: Bar cross-section area (mm^2)); K_4: Bar fiber factor (1.0 for CFRP and GFRP); K_5: Bar surface factor (1.0 for SC surfaces, 1.05 for HW surfaces); E_{FRP}: Modulus of elasticity for FRP bar (MPa); A_t: Area of transverse bars (mm^2); s, n: Spacing and number of transverse bars (mm); E_t: Modulus of elasticity for transverse bars (MPa); E_s: Elasticity modulus of steel; γ: Failure mode factor (2.5 for concrete cracking failure, 1.25 for pull-out failure).

Each formula's application range is determined based on the variation range of parameters in the underlying dataset used to formulate the respective equation. The formula specified in the ACI-440 provides a clear regulation on the scope of use. However, this clarity is lacking in the formulations of CSA, JSCE, or FIB. Despite this, to address the initial goal of studying the applicability of formulas across various FRP bars, as well as high and ultra-high-strength concrete, a wide range of experimental data has been considered in the comparison of calculated values and experimental results.

3.2. Correlation between formulas and experimental results

Figure 3 illustrates the relationship between the experimental bond strength values of FRP bars in concrete and the calculated bond strength values from the formulas proposed in Table 1 using a box plot. The blue box in Figure 3 represents the interquartile range, with the red line denoting the median value. The first percentile (Q1), encompassing 25% of values below the median, and the third percentile (Q3), encapsulating 75% of values above the median, form the top and bottom of the box, respectively. The whiskers outside the box extend to the minimum and maximum values of the dataset, while outliers beyond the whiskers are denoted by a red '+' symbol.

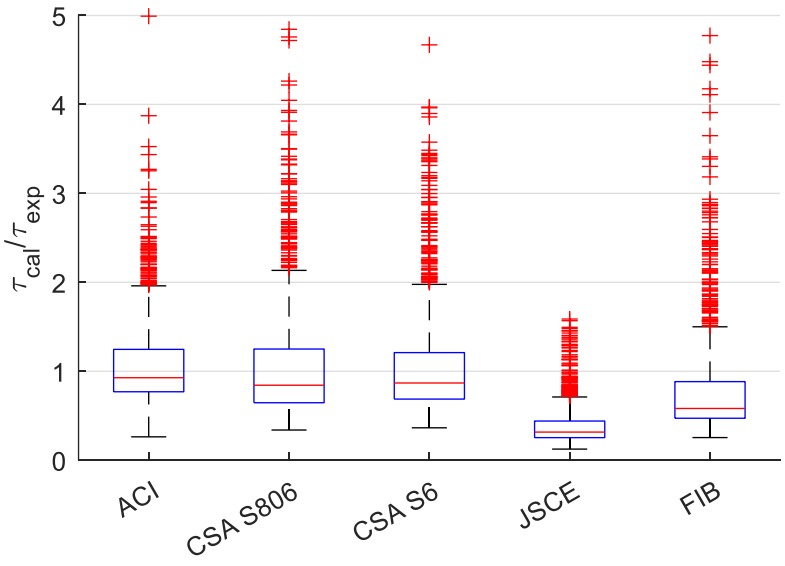

Figure 3. Correlation between experimental values and values of existing formulas.

In addition, Table 2 shows the results of regression analysis between calculated values of existing formulas and experimental data, which are measured in terms of RMSE and R^2,

$$RMSE = \sqrt{MSE} = \frac{1}{n}\sum_{i=1}^{n}(y_i - \hat{y}_i)^2 \text{ and } R^2 = 1 - \frac{\sum_{i=1}^{n}(y_i-\hat{y}_i)^2}{\sum_{i=1}^{n}(y_i-\bar{y})^2}, \quad (1)$$

where n is the number of observations, $\hat{y}_i$ is the predicted value of y_i, and $\bar{y}$ is the mean value of y_i.

Observing Figure 3 and Table 2, a substantial number of outliers are evident, indicating a weak correlation between the experimental values and the assessment results derived from the seven formulas in Table 1. This discrepancy is expected, as each formula is constructed on a limited dataset with a specific application scope. In this study, a dataset comprising 1010 specimens, inclusive of high and ultra-high strength concrete types, diverse bar diameters, and varied machined surfaces, was utilized. This diversity leads to out-of-range results for many of the proposed formulas. Most formulas in Table 1 yield an average value of less than 1, suggesting an underestimation of the bond strength compared to experimental values. Notably, the JSCE formula exhibits the smallest average value and standard deviation among the formulas, with a substantial difference from the value of 1.0. This is attributed to the JSCE formula primarily relying on concrete strength for bond strength calculation, neglecting other influential parameters.

Table 2. Regression analysis results between calculated values of existing formulas and experimental data.

Formulas	R^2	RMSE
ACI 440 1R – 06	0.382	5.747
CSA S806	0.125	8.621
CSA S6 – 06	0.190	7.432
JSCE	0.181	12.963
FIB	0.100	8.865

In conclusion, the analysis results indicate limitations in the currently proposed formulas in Table 1 when applied to evaluate the overall bond strength of FRP bars in concrete within a complex and diverse dataset. Consequently, there is a pressing need for the development of a more comprehensive model capable of considering the intricate influence of various parameters across a broad spectrum.

4. PREDICTION MODELS FOR BOND STRENGTH OF FRP BARS IN CONCRETE

4.1. Feature importance

Before constructing predictive models, an essential preliminary step involves evaluating the importance of each feature within the dataset.

The chosen method for feature selection is the F-test, where the F-statistic is computed by contrasting the variability between the means of distinct features against the variability within each feature. Despite the relatively modest scores assigned to FRP type and block length, their inclusion is deemed valuable. The outcomes indicate that even with a limited impact, these variables still play a role in influencing bond strength. To underscore the holistic nature of the prediction model, all 12 input variables have been retained for model development. This comprehensive approach ensures that the model accounts for all potential contributors, thereby enhancing its overall predictive capability.

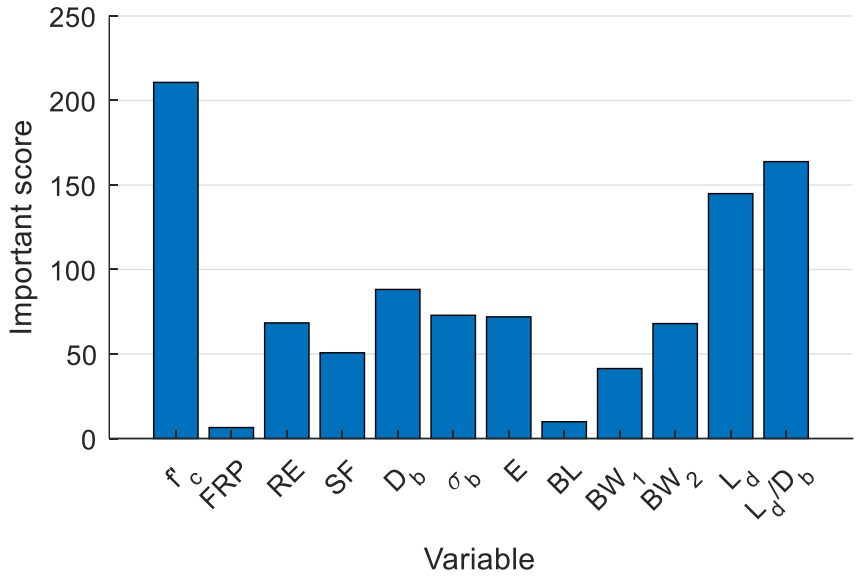

Figure 4. Feature selection results based on F-Test.

4.2. Multivariate linear regression model

MLR is a statistical modeling technique that enables the estimation of a dependent variable by considering two or more independent variables associated with the dependent variable. The form of the multivariate linear regression model is expressed as

$$Y = \beta_0 + \beta_1 X_1 + \beta_2 X_2 + \cdots + \beta_p X_p + \varepsilon, \quad (1)$$

in which, Y is the dependent variable, β_0 is the intercept term, β_1, β_2, ..., β_p are the coefficients of the independent variables X_1, X_2, ..., X_n, representing the strength and direction of their influence on the dependent variable.

To assess the multivariate linear regression model, the experimental dataset incorporates parameters such as bar type and polymer type, which are then digitized for thorough analysis and evaluation of the model. Within this model, the input independent variables encompass concrete compressive strength parameters, FRP reinforcement type, polymer resin type, bar diameter, bar durability limit, concrete block size, bar embedded length in concrete, and the ratio of bar embedded length and bar diameter. Moreover, the dependent variable in this context is the bond strength parameter derived from the experimental data.

The resulting equation uses an MLR model from MATLAB software given as

$$BS = 2.3870 + 0.1128 f_c' + 1.8008 FRP + 0.2946 RE + 0.0235 SF - 0.0322 D_b - 0.0020 \sigma_b + 0.0304 E + 0.0259 BL - 0.0671 BW_1 + 0.0909 - 0.0691 L_d + 0.0171 \frac{L_d}{D_b}, \quad (2)$$

where, f_c' represents the compressive strength of concrete (MPa), type of FRP bar (1: CFRP, 2: GFRP, and 3: BFRP), RE is type of polymeric resin (1: Vinylester, 2: Polyester, 3: Polyvinyl chloride, and 4: Epoxy), SF is the type of surface treatment method (1 is HW, 2 is SC, 3 is HW and SC), D_b is the bar diameter, σ_b is the durability limit of the bar (MPa), E is the elastic modulus (GPa), BL, BW_1 , BW_2 are the concrete specimen sizes (mm), L_d is the embedded

length of FRP bar in concrete (mm), L_d/D_b is the ratio of bar embedded length and bar diameter.

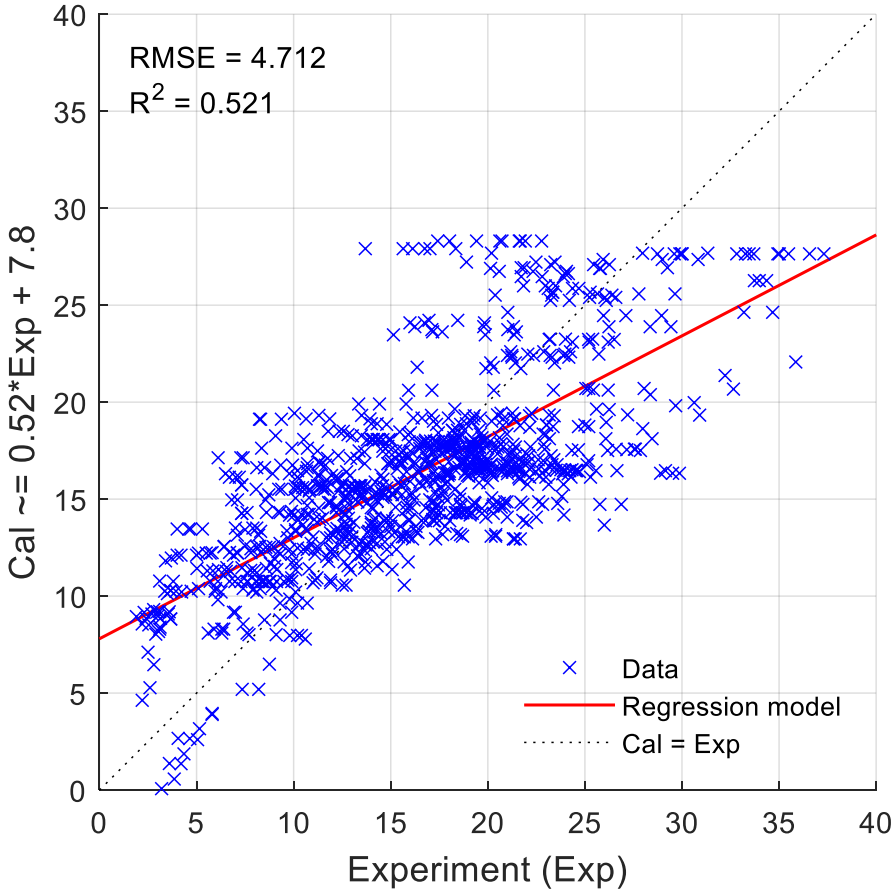

Figure 5. Predicted results compared with experimental results according to the multivariate regression model.

Figure 5 illustrates the accuracy of the MLR prediction results with the observed response from the dataset. The R^2 coefficient is calculated to be 0.521 and an RMSE value of 4.712, indicating a relatively low correlation. This might be attributed to the fact that the linear regression model, as represented, does not capture the nuanced and complex influence of the parameters on the bond strength between FRP bars and concrete. In essence, the current model treats the effects of parameters as entirely independent variables. However, interactions between parameters can manifest. For instance, the impact of bar diameter or the elastic modulus of FRP bars may vary across different types of concrete, and the effect of FRP bar burial length may differ for various test specimen sizes. Hence, there is a need for a more intricate model that can account for these interrelationships.

4.3. Artificial neural network model

4.3.1. ANN architecture

The ANN is a sophisticated mathematical model for information processing, inspired by the functioning of the biological nervous system, employing numerous interconnected neurons. An ANN network can be conceptualized as a highly parallel and distributed structure for

information processing. The performance of an ANN is contingent on various factors, including the neural network architecture, the input and output characteristics of each neuron, the training algorithm, and the learning data [61]. Consequently, the architecture of the neural network stands out as a crucial determinant of the learning capacity of the ANN network. Typically, the ANN architecture comprises three fundamental components: the input layer, hidden layer, and output layer, as illustrated in Figure 6.

Similarly, 12 parameters of the dataset in Section 4.1 are selected as input layer neurons. Only one node in the output layer is used to represent the bond strength between FRP reinforcement and concrete. In addition, feedforward neural network (FFNN) and cascade-forward neural network (CFNN) are deployed in this machine learning method. Among them, FFNN is widely used owing to its simple architecture and is easy to train.

Based on this architecture, a MATLAB-based program is developed. For the activation function, the hyperbolic tangent sigmoid function (tansig) is used. The Levenberg-Marquardt backpropagation is used as a train function, the maximum number of epochs is set as 1000, the performance function is MSE with a goal of 0, and the minimum gradient is 1.0×10^{-07}.

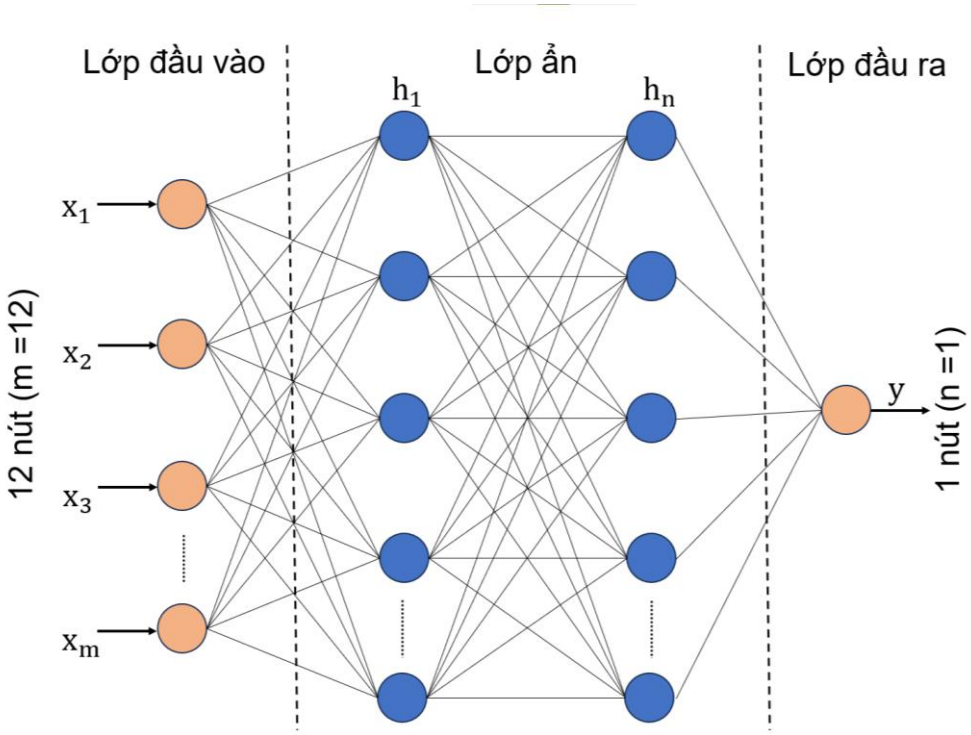

Figure 6. ANN network architecture.

4.3.2. Training and validation of ANN model

To construct a model for evaluating the bond strength of FRP bars in concrete, the dataset comprising 1010 test specimens is partitioned into three subsets with a ratio of 0.70:0.15:0.15, representing the training set, testing set, and validation set, respectively. Throughout the development of the ANN model, exploration is conducted on the number of neurons in a hidden layer and the number of hidden layers to ascertain the optimal ANN architecture that yields the best results. To evaluate this, the RMSE and R^2 values are adopted.

Table 3. Performance results of the parameter analysis.

ANN model	Number of hidden layers	Total training time (s)	No. of neurons per hidden layer	Training		Validation		Testing	
				R^2	RMSE	R^2	RMSE	R^2	RMSE
FFNN	1	66.0	20	0.905	2.124	0.920	1.758	0.887	2.315
	2	75.7	20	0.900	2.135	**0.934**	**1.746**	**0.915**	**2.043**
	3	93.8	18	0.907	2.066	0.927	1.711	0.911	2.181
CFNN	1	70.9	20	0.904	2.085	0.933	1.811	0.890	2.280
	2	88.2	10	0.913	1.995	**0.932**	**1.735**	**0.926**	**1.947**
	3	202.7	10	0.901	2.140	**0.940**	**1.503**	**0.932**	**1.916**

The implementation of the ANN model to assess the bond strength between the FRP bar and concrete involves training with both FFNN and CFNN. The architecture of these networks is configured with varying numbers of hidden layers, specifically 1, 2, and 3 hidden layers. Iterations are conducted for each case with the number of neurons in each hidden layer ranging from 2 to 20. Performance results as well as the total training time for each case are documented in Table 3. Examples of the performance comparison concerning the validation set of two networks are shown in Figure 7. Since the total training times are not much different, the validation of the models is mainly based on their performance measured by R^2 and RMSE. It is observed that the optimal number of neurons in a hidden layer for the FFNN in the three cases is determined to be 20, 20, and 18, respectively, while the CFNN has optimal neuron numbers 20, 10, and 10, respectively for 1, 2, and 3 hidden layers. It is noticed that the optimal network architecture is chosen based on the performance measured by the validation and test sets.

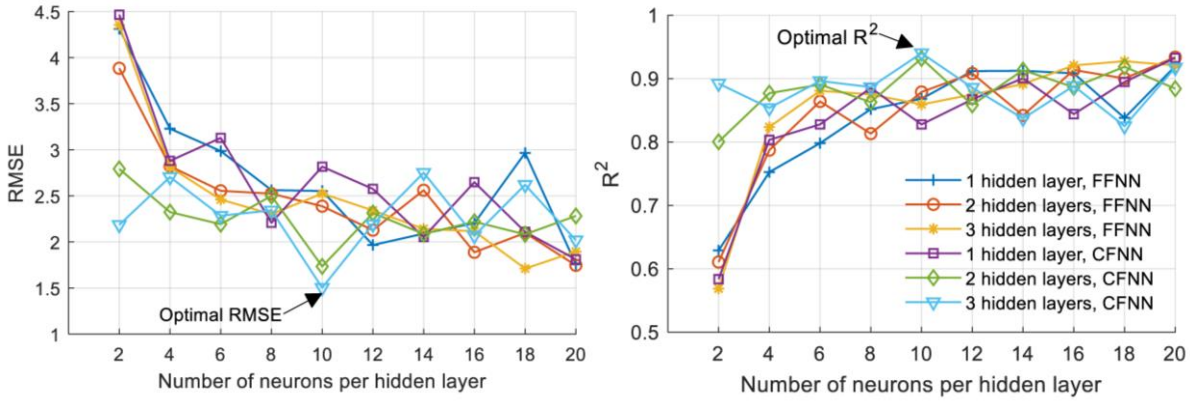

(a) R^2 value *(b) RMSE value*

Figure 7. Performance of the FFNN and CFNN models according to the number of hidden layers and number of neurons per hidden layer.

Based on the insights gleaned from the analysis presented in Table 3, it becomes evident that the FFNN model, characterized by two hidden layers, each housing 20 neurons, outshines the others in performance metrics. It achieves the highest R^2 value and the smallest RMSE value for both the validation and test sets, highlighted in bold, underscoring its superior predictive accuracy. On the other side, the CFNN featuring the configurations of two and three hidden layers, each with 10 neurons, also emerges as a strong performer. They yield notable R^2 values more than 0.92 and RMSE values less than 1.95, showcasing commendable predictive capabilities.

The consistently elevated performance across both validation and test sets attests to the robustness of the models, emphasizing their superiority when compared to the above MLR model and the existing formulas in terms R^2 and RMSE. This underscores the efficacy and reliability of the proposed models in predicting bond strength, making them a valuable advancement in the field.

5. CONCLUSIONS

In this study, a large dataset comprising 1010 pull-out test specimens of FRP bars in concrete considering various experimental parameters was collected from 32 studies with the aims of evaluating existing formulas in the codes and developing more accurate models, based on MLR and ANN models, for the bond strength of FRP bars in concrete. The findings from the study are summarized as follows:

- The study results reveal a low correlation between the existing formulas and the extensive experimental dataset collected. This is attributed to each formulation being constructed on a limited dataset, whereas the dataset used in this study comprises 1010 specimens, encompassing high and ultra-high strength concretes, diverse types of FRP bars, and various machined surfaces. These factors contribute to out-of-range predictions in many of the proposed formulas.

- The multivariate linear regression model demonstrates relatively low accuracy in predicting the bond strength of FRP bars in concrete. This inadequacy is attributed to the linear regression model's failure to capture the complex interplay of parameters influencing the bond strength between FRP bars and concrete.

- Two different ANN models were developed, FFNN and CFNN. A parametric study was also conducted to achieve the optimal architecture of the models. It is concluded that both FFNN and CFNN models yield high performance compared with the MLR model and the existing formulas, featuring optimized architectures with 2 hidden layers with 20 neurons in each hidden layer for the FFNN and 2 and 3 hidden layers with 10 neurons per hidden layer for the CFNN.

- It is a highlight that, when considering a broader range of applications, the ANN serves as a robust tool for accurately predicting the bond strength of FRP bars in concrete, in comparison to traditional formulas and linear regression models. This assessment approach provides engineers with a convenient, high-precision tool for designs utilizing various forms of FRP bars and diverse types of concrete in practical design scenarios.

ACKNOWLEDGMENT

This work is funded by The University of Danang - University of Science and Technology under project code B2022-DN02-10.

REFERENCES

[1]. X. Zou, H. Lin, P. Feng, Y. Bao, J. Wang, A review on FRP-concrete hybrid sections for bridge applications, Composite Structures, 262 (2021) 113336. https://doi.org/10.1016/j.compstruct.2020.113336.
[2]. Y. M. Amran, R. Alyousef, R. S. Rashid, H. Alabduljabbar, C. C. Hung, Properties and applications of FRP in strengthening RC structures: A review, Structures, 16 (2018) 208-238. https://doi.org/10.1016/j.istruc.2018.09.008
[3]. S. M. Hosseini, M. Yekrangnia, A. V. Oskouei, Effect of spiral transverse bars on structural

behavior of concrete shear walls reinforced with GFRP bars, Journal of Building Engineering, 55 (2022) 104706. https://doi.org/10.1016/j.jobe.2022.104706
[4]. H. A. Hasan, M. N. Sheikh, M. N. Hadi, Maximum axial load carrying capacity of Fibre Reinforced-Polymer (FRP) bar reinforced concrete columns under axial compression, Structures, 19 (2019) 227-233. https://doi.org/10.1016/j.istruc.2018.12.012
[5]. X. Hu, J. Xiao, K. Zhang, Q. Zhang, The state-of-the-art study on durability of FRP reinforced concrete with seawater and sea sand, Journal of Building Engineering, 51 (2022) 104294. https://doi.org/10.1016/j.jobe.2022.104294
[6]. A. Confrere, L. Michel, E. Ferrier, G. Chanvillard, Experimental behaviour and deflection of low-strength concrete beams reinforced with FRP bars, Structural Concrete, 17 (2016) 858-874. https://doi.org/10.1002/suco.201500046
[7]. F. Aslani, S. Nejadi, Bond behavior of reinforcement in conventional and self-compacting concrete, Advances in Structural Engineering, 15 (2012) 2033-2051. https://doi.org/10.1260/1369-4332.15.12.2033
[8]. X. Lin, Y. Zhang, Evaluation of bond stress-slip models for FRP reinforcing bars in concrete, Composite Structures, 107 (2014) 131-141. https://doi.org/10.1016/j.compstruct.2013.07.037
[9]. R. J. Hamad, M. M. Johari, R. H. Haddad, Mechanical properties and bond characteristics of different fiber reinforced polymer rebars at elevated temperatures, Construction and Building Materials, 142 (2017) 521-535. https://doi.org/10.1016/j.conbuildmat.2017.03.113
[10]. L. Xiao, S. Dai, Q. Jin, S. Peng, Bond performance of GFRP bars embedded in steel-PVA hybrid fiber concrete subjected to repeated loading, Structural Concrete, 24 (2023) 1597-1611. https://doi.org/10.1002/suco.202100607
[11]. A. Nanni, A. De Luca, H. J. Zadeh, Reinforced concrete with FRP bars: Mechanics and design. CRC press, 2014.
[12]. R. Sun, R. Perera, J. Gu, Y. Wang, A simplified approach for evaluating the flexural response of concrete beams reinforced with FRP bars, Frontiers in Materials, 8 (2021) 765058. https://doi.org/10.3389/fmats.2021.765058
[13]. Q. Li, M. Fu, B. Xie, Analyzing the bond behavior of Fiber-Reinforced Polymer (FRP) bars embedded in Engineered Cementitious Composites (ECCs) with the nonlocal continuum rod model, Mathematical Problems in Engineering, 2020 (2020) 1-12. https://doi.org/10.1155/2020/1710364
[14]. M. H. Omrani, M. Dehestani, H. Yousefpour, Flexural behavior of lightweight concrete beams reinforced with GFRP bars and prestressed with steel strands, Structural Concrete, 22 (2021) 69-80. https://doi.org/10.1002/suco.201900342
[15]. R. Okelo, R. L. Yuan, Bond strength of fiber reinforced polymer rebars in normal strength concrete, Journal of Composites for Construction, 9 (2005) 203-213. https://doi.org/10.1061/(ASCE)1090-0268(2005)9:3(203)
[16]. J. Y. Lee, T. Y. Kim, T. J. Kim, C. K. Yi, J. S. Park, Y. C. You, Y. H. Park, Interfacial bond strength of glass fiber reinforced polymer bars in high-strength concrete, Composites Part B: Engineering, 39 (2008) 258-270. https://doi.org/10.1016/j.compositesb.2007.03.008
[17]. Guide for the Design and Construction of Structural Concrete Reinforced with FRP Bars, American Concrete Institute, USA, 2006.
[18]. Design and Construction of Building Components with Fibre-Reinforced Polymers, Canadian Standards Association, Canada, 2012.
[19]. Canadian Highway Bridge Design Code, Canadian Standards Association, Canada, 2006.
[20]. A. Machida, T. Uomoto, Recommendation for design and construction of concrete structures using continuous fiber reinforcing materials, Japan Society of Civil Engineers, Japan, 1997.
[21]. M. Code, First Complete Draft-Volume 2: Model Code; Fédération Internationale du Béton (FIB), Switzerland, 2010.
[22]. N. C. Concha, Neural network model for bond strength of FRP bars in concrete, Structures, 41 (2022) 306-317. https://doi.org/10.1016/j.istruc.2022.04.088
[23]. B. Basaran, I. Kalkan, E. Bergil, E. Erdal, Estimation of the FRP-concrete bond strength with code formulations and machine learning algorithms, Composite Structures, 268 (2021) 113972.

https://doi.org/10.1016/j.compstruct.2021.113972
[24]. H. Kazemi, M. Yekrangnia, M. Shakiba, M. Bazli, A. Vatani Oskouei, Bond durability between anchored GFRP bar and seawater concrete under offshore environmental conditions, Materials and Structures, 56 (2023) 64. https://doi.org/10.1617/s11527-023-02153-5
[25]. E. Toumpanaki, J. M. Lees, G. P. Terrasi, Bond durability of carbon fiber–reinforced polymer tendons embedded in high-strength concrete, Journal of Composites for Construction, 22 (2018) 04018032. https://doi.org/10.1061/(ASCE)CC.1943-5614.0000870
[26]. X. Liu, X. Wang, K. Xie, Z. Wu, F. Li, Bond behavior of basalt fiber-reinforced polymer bars embedded in concrete under mono-tensile and cyclic loads, International Journal of Concrete Structures and Materials, 14 (2020) 1-15. https://doi.org/10.1186/s40069-020-0394-4
[27]. M. Ekenel, Fiber Reinforced Polymer Reinforcement for Concrete Members-ACI Committee 400 is taking the next step toward building code compliance, Concrete International, 43 (2021) 52-56.
[28]. A. Parghi, M. S. Alam, A review on the application of sprayed-FRP composites for strengthening of concrete and masonry structures in the construction sector, Composite Structures, 187 (2018) 518-534. https://doi.org/10.1016/j.compstruct.2017.11.085
[29]. Y. Liu, Z. H. Tao, Z. H. Hao, L. Lu, H. M. Yang, W. J. Cai, S. Guan, Experimental study on mechanical properties of novel FRP bars with hoop winding layer, Advances in Materials Science and Engineering, (2021) 1-18. https://doi.org/10.1155/2021/9554687
[30]. M. Baena, L. Torres, A. Turon, C. Barris, Experimental study of bond behaviour between concrete and FRP bars using a pull-out test, Composites Part B: Engineering, 40 (2009) 784-797. https://doi.org/10.1016/j.compositesb.2009.07.003
[31]. B. Basaran, I. Kalkan, Development length and bond strength equations for FRP bars embedded in concrete, Composite Structures, 251 (2020) 112662. https://doi.org/10.1016/j.compstruct.2020.112662.
[32]. A. Katz, Bond mechanism of FRP rebars to concrete, Materials and Structures, 32 (1999) 761-768. https://doi.org/10.1007/BF02905073
[33]. A. Rolland, M. Quiertant, A. Khadour, S. Chataigner, K. Benzarti, P. Argoul, Experimental investigations on the bond behavior between concrete and FRP reinforcing bars, Construction and building Materials, 173 (2018) 136-148. https://doi.org/10.1016/j.conbuildmat.2018.03.169
[34]. S. Islam, H. M. Afefy, K. Sennah, H. Azimi, Bond characteristics of straight-and headed-end, ribbed-surface, GFRP bars embedded in high-strength concrete, Construction and Building Materials, 83 (2015) 283-298. https://doi.org/10.1016/j.conbuildmat.2015.03.025
[35]. Z. Achillides, K. Pilakoutas, Bond behavior of fiber reinforced polymer bars under direct pullout conditions, Journal of Composites for construction, 8 (2004) 173-181. https://doi.org/10.1061/(ASCE)1090-0268(2004)8:2(173)
[36]. L. J. Malvar, J. Cox, K. B. Cochran, Bond between carbon fiber reinforced polymer bars and concrete. I: Experimental study, Journal of Composites for Construction, 7 (2003) 154-163. https://doi.org/10.1061/(ASCE)1090-0268(2003)7:2(154)
[37]. A. Belarbi, H. Wang, Bond durability of FRP bars embedded in fiber-reinforced concrete, Journal of Composites for Construction, 16 (2012) 371-380. https://doi.org/10.1061/(ASCE)CC.1943-5614.0000270
[38]. Z. Dong, G. Wu, B. Xu, X. Wang, L. Taerwe, Bond durability of BFRP bars embedded in concrete under seawater conditions and the long-term bond strength prediction, Materials & Design, 92 (2016) 552-562. https://doi.org/10.1016/j.matdes.2015.12.066
[39]. W. Wei, F. Liu, Z. Xiong, Z. Lu, L. Li, Bond performance between fibre-reinforced polymer bars and concrete under pull-out tests, Construction and Building Materials, 227 (2019) 116803.
[40]. W. Tang, T. Lo, R. V. Balendran, Bond performance of polystyrene aggregate concrete (PAC) reinforced with glass-fibre-reinforced polymer (GFRP) bars, Building and Environment, 43 (2008) 98-107. https://doi.org/10.1016/j.buildenv.2006.11.030
[41]. A. Abbasi, P. J. Hogg, Temperature and environmental effects on glass fibre rebar: modulus, strength and interfacial bond strength with concrete, Composites Part B: Engineering, 36 (2005) 394-404. https://doi.org/10.1016/j.compositesb.2005.01.006
[42]. B. Tighiouart, B. Benmokrane, D. Gao, Investigation of bond in concrete member with fibre

reinforced polymer (FRP) bars, Construction and Building Materials, 12 (1998) 453-462. https://doi.org/10.1016/S0950-0618(98)00027-0
[43]. M. Bazli, H. Ashrafi, A. V. Oskouei, Experiments and probabilistic models of bond strength between GFRP bar and different types of concrete under aggressive environments, Construction and Building Materials, 148 (2017) 429-443. https://doi.org/10.1016/j.conbuildmat.2017.05.046
[44]. Y. Ding, X. Ning, Y. Zhang, F. P. Torgal, J. Aguiar, Fibres for enhancing of the bond capacity between GFRP rebar and concrete, Construction and Building Materials, 51 (2014) 303-312. https://doi.org/10.1016/j.conbuildmat.2013.10.089
[45]. J. F. Davalos, Y. Chen, I. Ray, Effect of FRP bar degradation on interface bond with high strength concrete, Cement and Concrete Composites, 30 (2008) 722-730. https://doi.org/10.1016/j.cemconcomp.2008.05.006
[46]. J. P. Won, C. G. Park, H. H. Kim, S. W. Lee, C. I. Jang, Effect of fibers on the bonds between FRP reinforcing bars and high-strength concrete, Composites Part B: Engineering, 39 (2008) 747-755. https://doi.org/10.1016/j.compositesb.2007.11.005
[47]. J. Zhou, X. Chen, S. Chen, Effect of different environments on bond strength of glass fiber-reinforced polymer and steel reinforcing bars, KSCE Journal of Civil Engineering, 16 (2012) 994-1002.
[48]. M. Robert, B. Benmokrane, Effect of aging on bond of GFRP bars embedded in concrete, Cement and Concrete Composites, 32 (2010) 461-467. https://doi.org/10.1007/s12205-012-1462-3
[49]. Q. Hao, Y. Wang, Z. He, J. Ou, Bond strength of glass fiber reinforced polymer ribbed rebars in normal strength concrete, Construction and Building Materials, 23 (2009) 865-871. https://doi.org/10.1016/j.conbuildmat.2008.04.011
[50]. A. Godat, S. Aldaweela, H. Aljaberi, N. Al Tamimi, E. Alghafri, Bond strength of FRP bars in recycled-aggregate concrete, Construction and Building Materials, 267 (2021) 120919. https://doi.org/10.1016/j.conbuildmat.2020.120919
[51]. M. Antonietta Aiello, M. Leone, M. Pecce, Bond performances of FRP rebars-reinforced concrete, Journal of Materials in Civil Engineering, 19 (2007) 205-213. https://doi.org/10.1061/(ASCE)0899-1561(2007)19:3(205)
[52]. K. Hossain, D. Ametrano, M. Lachemi, Bond strength of standard and high-modulus GFRP bars in high-strength concrete, Journal of Materials in Civil Engineering, 26 (2014) 449-456. https://doi.org/10.1061/(ASCE)MT.1943-5533.0000758
[53]. B. Kim, J. H. Doh, C. K. Yi, J. Y. Lee, Effects of structural fibers on bonding mechanism changes in interface between GFRP bar and concrete, Composites Part B: Engineering, 45 (2013) 768-779. https://doi.org/10.1016/j.compositesb.2012.09.039
[54]. I. Vilanova, M. Baena, L. Torres, C. Barris, Experimental study of bond-slip of GFRP bars in concrete under sustained loads, Composites Part B: Engineering, 74 (2015) 42-52. https://doi.org/10.1016/j.compositesb.2015.01.006
[55]. F. Yan, Z. Lin, D. Zhang, Z. Gao, M. Li, Experimental study on bond durability of glass fiber reinforced polymer bars in concrete exposed to harsh environmental agents: Freeze-thaw cycles and alkaline-saline solution, Composites Part B: Engineering, 116 (2017) 406-421. https://doi.org/10.1016/j.compositesb.2016.10.083
[56]. Y. Gong, J. Song, Y. Zhang, The interfacial bond properties and model for basalt fiber reinforced polymer bar in ultra-high-performance concrete subjected monotonic and reversed cyclic loading, Journal of Building Engineering, 72 (2023) 106606. https://doi.org/10.1016/j.jobe.2023.106606
[57]. D. Tong, Y. Chi, L. Huang, Y. Zeng, M. Yu, L. Xu, Bond performance and physically explicable mathematical model of helically wound GFRP bar embedded in UHPC, Journal of Building Engineering, 69 (2023) 2352-7102. https://doi.org/10.1016/j.jobe.2023.106322
[58]. J. J. Zeng, J. J. Liao, Y. Zhuge, Y. C. Guo, J. K. Zhou, Z. H. Huang, L. Zhang, Bond behavior between GFRP bars and seawater sea-sand fiber-reinforced ultra-high strength concrete, Engineering Structures, 254 (2022) 113787. https://doi.org/10.1016/j.engstruct.2021.113787
[59]. F. Soltanzadeh, A. E. Behbahani, E. N. Pereira, Bond behavior of recycled tyre steel fiber reinforced concrete and basalt fiber-reinforced polymer bars under static and fatigue loading conditions, Journal of Building Engineering, 70 (2023) 106291. https://doi.org/10.1016/j.engstruct.2021.113787
[60]. L. Ke, L. Liang, Z. Feng, C. Li, J. Zhou, Y. Li, Bond performance of CFRP bars embedded in

UHPFRC incorporating orientation and content of steel fibers, Journal of Building Engineering, 73 (2023) 106827. https://doi.org/10.1016/j.jobe.2023.106291
[61]. N. D. Lagaros, Artificial Neural Networks Applied in Civil Engineering, Applied Sciences, 13 (2023) 1131. https://doi.org/10.3390/app13021131